



Contents lists available at ScienceDirect



Catalysis Today

journal homepage: www.elsevier.com/locate/cattod

Effect of redox properties of LaCoO₃ perovskite catalyst on production of lactic acid from cellulosic biomass

Xiaokun Yang^a, Lisha Yang^a, Wei Fan^b, Hongfei Lin^{a,*}

^a Department of Chemical and Materials Engineering, University of Nevada, 1664 N. Virginia St., Reno, NV 89557, USA

^b Department of Chemical Engineering, University of Massachusetts Amherst, 686 N. Pleasant Street, Amherst, MA 01002, USA

ARTICLE INFO

Article history:

Received 1 August 2015

Received in revised form

30 November 2015

Accepted 21 December 2015

Available online xxx

Keywords:

Glucose

Xylose

Cellulose

Lactic acid

Perovskite

Redox catalysis

ABSTRACT

Cost-effective conversion of cellulosic biomass to value-added lactic acid with heterogeneous catalysts has attracted much attention recent years. While both solid Lewis acids and bases have been extensively studied, the role of redox catalysts for the production of lactic acid is barely understood. Herein, the LaCoO₃ perovskite metal oxides with strong redox properties and a good stability in hydrothermal media were used as the catalysts for the conversion of a variety of cellulosic biomass to lactic acid. The effects of reaction conditions such as reaction temperature, catalyst loading, and gas atmosphere were investigated. At the optimum conditions, the yields of approximately 40%, 38%, and 24% lactic acid were obtained from glucose, xylose and cellulose, respectively. The key intermediates such as pyruvic acid were used as the probe reactants to explore the reaction mechanism. Unlike Lewis acid or base catalysed sugar conversion reactions, the redox pathway might start from the oxidative decarboxylation of aldose sugars and the lattice oxygen atoms in the LaCoO₃ perovskite structure participate the redox cycles in the conversion of sugars to lactic acid. Lastly, the stability of the LaCoO₃ catalyst in hydrothermal reaction media was discussed.

© 2016 Elsevier B.V. All rights reserved.

1. Introduction

With the gradual depletion of fossil fuels and the increasing concern of greenhouse gas emissions linked to climate change, using biomass resources instead of petroleum to manufacture commodity chemicals has attracted growing interest in recent years [1,2]. Carbohydrates, the most abundant biomass compounds, are a sustainable feedstock which can be used to produce bio-based platform chemicals [3]. Lactic acid (LA) is such a sugar derived platform chemical that can be converted into a wide range of useful compounds [3–5]. Its global production capacity is over 500,000 tons per year and continues to grow [5]. Currently, the commercial production of LA is via fermentation processes which have drawbacks such as slow kinetics, poor scalability, and large amounts of waste [6,7].

Various chemo-catalytic processes have been studied other than the industrial fermentation to produce lactic acid [8,9]. Jin's group synthesized lactic acid with a 27% yield from glucose in a 2.5 M NaOH hydrothermal solution [10]. Epane et al. produced lactic acid in a 75C-% yield using KOH as the catalyst via the microwave-

assisted method [11]. However, strong homogeneous mineral base catalysts can cause severe corrosion, and thus limiting their use in lactic acid production. Therefore, the development of highly effective heterogeneous catalysts for converting carbohydrates to LA is highly desirable. Champon et al. reported that the yields of 27 mol-% and 18 mol-% of LA were produced from cellulose over tungstated zirconia (ZrW) and tungstated alumina (AlW), respectively, in subcritical water [12]. Taarning's group used Sn-beta as the Lewis acid catalyst and obtained a 26C-% yield of LA from glucose at in aqueous media [13]. Our group found that the yields of 42 mol-% and 30 mol-% of LA were obtained from xylose and xylan, respectively, using the ZrO₂ catalyst [14]. Wang et al. used CuO as an oxidant to convert glucose to lactic acid in the yield of 59 mol-% in alkaline solution [15]; however, CuO was reduced to Cu after the reaction. Dong's group recently reported a 67.6C-% yield of LA from cellulose with the erbium-exchanged montmorillonite K10 catalyst [16]. However, significant leaching of Er ions was observed. Several research groups [13,17–19] reported the conversion of carbohydrate biomass into lactic acid derivatives in organic solvents, in which leaching of metal oxide catalysts may be mitigated. Liu et al. found that with the solid base catalyst, MgO, ~29.5 mol-% methyl lactate was yielded from glucose in the methanol solvent [20]. However, most heterogeneous catalysts reported in literature for chemo-catalytic conversion of biomass to LA or lactates are based

* Corresponding author. Tel.: +1 7757844697; fax: +1 7753275059.

E-mail address: HongfeiL@unr.edu (H. Lin).

on acid/base properties. Long-term stabilities of these catalysts are still uncertain due to leaching or deactivation in hydrothermal media.

The stability issue of transition metal oxide materials in hydrothermal media has been the concern plaguing the aqueous-phase catalysis. Only few metal oxides (such as ZrO_2 , TiO_2 and $\alpha-Al_2O_3$) exhibit acceptable stabilities in certain biomass conversion reactions in subcritical water [21–24]. Developing mixed metal oxide catalysts could improve the stability of heterogeneous catalysts. For instance, perovskite materials, composed of mixed transition metal ions with lanthanides, exhibit better stabilities compared to single metal oxides in certain catalytic reactions [25,26]. The redox properties of perovskite metal oxides catalysed a variety of reactions including CO oxidation [27], CO_2 reforming [28–31], NO oxidation [32–34], and oxidation of hydrocarbons [25,35–37]. Recently, Deng et al. found that the perovskite metal oxides, such as $LaMnO_3$, $LaCoO_3$, $LaFe_{1-x}Cu_xO_3$, etc., were efficient catalysts for the wet aerobic oxidation of lignin to aromatic aldehydes [38–40]. Escalona et al. used $La_{1-x}Ce_xNiO_3$ to convert guaiacol to cyclohexanol with a yield of 60% [41]. Li et al. [42] found that Cr modified $LaCo_{0.8}Cu_{0.2}O_3$, catalysed the production of furfural from xylan at 160 °C. To the best of our knowledge, the application of perovskite oxide catalysts in the LA production is rarely reported.

Herein, we report that the $LaCoO_3$ perovskite oxide is an efficient heterogeneous catalyst for the conversion of cellulosic biomass to LA. For the first time, we found that the redox properties of the $LaCoO_x$ catalyst, which is distinctly different from the acid/base properties of the prevailing catalysts for the LA production, play a central role in the conversion of a variety of C3–C6 aldose sugars and their polysaccharides to LA in subcritical water.

2. Experimental

2.1. Materials

The following reagents and products were used as received: D-(+)-xylose (99%), D-(+)-glucose (Reagent ACS Grade) and microcrystalline cellulose were purchased from Acros Organics. L-(+)-lactic acid (98%), lanthanum nitrate hexahydrate (98%), cobalt nitrate hexahydrate (98%), fructose (99%), sucrose (99%), lanthanum(III) oxide (99.9%), cobalt (II, III) oxide (99.5%) and citric acid (99%) were purchased from Sigma-Aldrich.

2.2. Catalyst preparation

In the typical synthesis, 0.2 mol $La(NO_3)_3 \cdot 6H_2O$ and 0.2 mol $Co(NO_3)_2 \cdot 6H_2O$ were dissolved into 50 mL DI water and stirred for 10 min. Then, 0.6 mol citric acid was added into the above solution and stirred for another 30 min. After that, the solution was placed into a wide mouth container and dried at 110 °C in an oven overnight. The dried powder was collected and heated to 200 °C at 10 °C/min for 30 min, then heated to 900 °C with the temperature ramp of 3 °C/min, and finally calcined at 900 °C for 4 h.

2.3. Catalyst characterization

A PANalytical X'Pert PRO diffractometer with graphite-filtered $Cu K\alpha$ radiation was used to determine the crystalline phases of the as-synthesized $LaCoO_3$ powder over the 2θ values from 10° to 90° with the step size of 0.02°.

H_2 temperature-programmed reduction (TPR) and O_2 temperature-programmed (TPO) on the catalysts were carried out using a Micromeritics AutoChem II 2920 Chemisorption Analyzer. In a typical H_2 TPR experiment, the catalyst was first degassed in helium at 900 °C for 1 h, following which the temperature was decreased to 30 °C in helium flow. Afterwards, the gas

flow was switched to 10% hydrogen in argon at 50 mL/min and the TPR was performed from 50 °C to 800 °C with the temperature ramp of 30 °C/min. Then, the sample was cooled to 30 °C in helium flow before the gas flow was switched to 10% oxygen in helium at 50 mL/min. TPO experiment was performed from 50 °C to 800 °C with the same temperature ramp of 30 °C/min.

Temperature-programmed desorption (TPD) of adsorbed NH_3 on the catalysts was carried out using the same Chemisorption Analyser. In a typical NH_3 TPD experiment, the catalyst was first degassed at 900 °C for 1 h and then cooled to 100 °C in a helium flow. Afterwards, the gas was switched to 10% ammonia in helium at the flow rate of 50 mL/min to allow NH_3 adsorption for 40 min. The physisorbed NH_3 was removed under helium flow for 30 min. The NH_3 TPD was performed from 50 °C to 800 °C with the temperature ramp of 30 °C/min.

The Bruker EQUINOX 55 Fourier transform infrared spectroscopy (FT-IR) spectrometer with a MCT detector was used for the characterization. The sample was loaded in a high-temperature reaction cell (Harrick) located within a DRIFT accessory (Praying MantisTM, Harrick). The sample was degassed at 550 °C for 1 h under helium in order to remove adsorbed water. After that, FT-IR spectra (with a resolution of 2 cm^{-1}) were collected from the sample at 120 °C. For pyridine adsorption, small aliquots of pyridine were subsequently exposed to the sample at 120 °C for 15 min. Prior to the measurement the weakly adsorbed pyridine was removed by flowing helium at 250 °C for 1 h, and the spectra were then collected at 120 °C.

Scanning electron microscopy with energy-dispersive X-ray spectroscopy (SEM-EDS) analyses have been carried out using a FEI Quanta 400 scanning electron microscope (Hillsboro, OR) equipped with a Thermo NSS-UPS-SEM-INORAN System SIX (Thermo Fisher Scientific, Waltham, MA) for X-ray microanalysis (EDS). For EDS analysis, the samples were placed on a stub with carbon tape and the SEM imaging was run at 15 kV. Aqueous solutions collected after reactions were analyzed by an Optima 3000 DV inductively coupled plasma atomic emission spectrometer (ICP-AES) (Acme Analytical Laboratory). All samples for ICP-AES analysis were acidified with 5% Optima HNO_3 .

2.4. Catalytic reaction procedure

Reactions were carried out by suspending the catalyst in a solution of biomass substrates in DI water in a 100 mL stirred Parr microreactor. In each reaction, a glass liner was used to prevent reactants from contacting the metal reactor walls. The liner was loaded and placed inside the reactor, and the reactor was charged with 400 psi N_2 . The reactor was heated at a ramp rate of 10 °C/min until the desired set temperature was reached. During the reaction, mixing was achieved through an internal propeller operating at 750 RPM. Once the set temperature was attained, the reactor was held at the set temperature for 1 h and then quenched in an ice bath for fast cooling. The reactor was then immediately disassembled and the solid residue was collected for calculation of mass conversion. The liquid and solid fractions were separated using a centrifuge. The liquid fraction was collected and used for subsequent chemical analysis and the solid residues were dried over night at 110 °C. The mass balance was calculated and ensured to be between 98% and 102%.

The conversion (X), solid residue yield (S.R.) and the product yield C-% (Y) are calculated using the following equations:

$$X = \left(1 - \frac{\text{mass of carbon in unreacted biomass}}{\text{mass of carbon in total biomass}} \right) \times 100\%$$

$$S.R. = \left(\frac{\text{Weight of total dried solid residue} - \text{Weight of solid catalyst}}{\text{Initial weight of biomass}} \right) \times 100\%$$

$$Y = \frac{\text{mass of carbon in product}}{\text{mass of carbon in total biomass}} \times 100\%$$

2.5. Stability study

For the catalyst stability tests, the spent catalyst was collected and dried overnight in an oven at 100 °C, and was further calcined in air at 550 °C for 6 h before reuse. For each run, there was a ~2% catalyst weight loss during the collection and transfer of the catalyst. The as-received regenerated catalysts were used for the subsequent reaction tests without adding supplemental fresh catalyst for all the catalyst stability tests. We kept the same amount of glucose loading for the first 3 times reuses, while slightly lowered the feeding amount of glucose to maintain the same molar ratio of glucose to catalyst in the 4th and 5th runs as that in the initial run.

2.6. Chemical analysis/characterization of products

The aqueous phase samples after reaction were filtered through a 0.45 micron syringe filter then diluted 10 times with the internal standard solution (200 ppm benzoic acid solution). High performance liquid chromatography (HPLC) was used for quantitative chemical analysis using a Shimadzu HPLC LC-10A system equipped with a UV-vis detector (Shimadzu SPD 10-AV) and a refractive index detector (Shimadzu RID-10A). For analysis of organic acids and reaction intermediates, the samples were separated in an Aminex HPX-87H Ion Exclusion column (Bio-Rad), using 5 mM H₂SO₄ as the mobile phase at a flow rate of 0.7 mL/min, and a column temperature of 55 °C. The wavelength of the UV-vis detector was set at 208 nm and 290 nm.

Qualitative gas chromatography coupled with mass spectrometry (GC-MS) analysis was performed for identification of unknown aqueous-phase products. The silylation derivatization method was reported before [14]. The derivatized samples were analysed by the Agilent 6890 series GC-MS equipped with a DB5-MS column (30 m × 0.25 mm ID, 0.25 um film thickness) and an Agilent 5973 mass selective detector. The column temperature was maintained at 80 °C for 2 min then ramped at 10 °C/min to 260 °C and held at 260 °C for 2 min.

3. Results and discussion

3.1. Catalytic effect of LaCoO₃ on glucose conversion

The crystalline rhombohedral perovskite structure of the as-synthesized LaCoO₃ catalyst was confirmed by the X-ray diffraction characterization (Fig. 1a). The characteristic spectrum of the sample showed the diffraction lines located at 2θ = 32.98°, 33.38° and 47.58° (JCPDS data no. 48-0123). No peaks related to bulk Co₃O₄ or La₂O₃ phases were detected.

Glucose conversions were compared with and without the LaCoO₃ catalyst at 200 °C in the pH neutral aqueous solutions (Entries 1 and 4, Table 1). The catalytic effect of the LaCoO₃ catalyst was obvious. Without a catalyst, the yield of LA was only 0.9%, while a 29.1% yield of 5-hydroxymethylfurfural (HMF) was formed which might be attributed to the acidic property of hydrothermal water [15]. Other carboxylic acids with short carbon chains like glycolic acid and acetic acid were produced with the total yield of less than 5%. In contrast, with the LaCoO₃ catalyst and under the otherwise identical reaction conditions, the yield of LA reached 39.5%. The carbon distribution of other acids also changed considerably: more acetic acid, ~4%, was produced compared to the catalyst-free reaction and especially, the yield of pyruvic acid was noticeable at 2.7%. Meanwhile, the yield of HMF decreased significantly to only

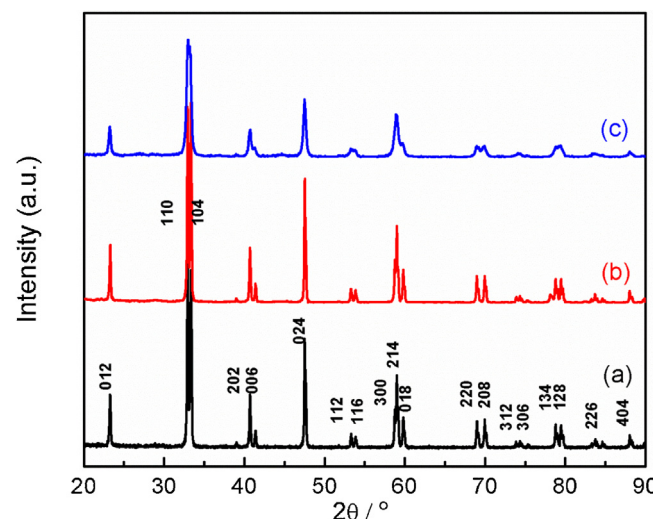


Fig. 1. XRD spectra of the LaCoO₃ structures: (a) fresh synthesized sample; (b) after 1 h hydrothermal treatment; (c) after 1 h reaction. Reaction conditions: 1 mmol glucose, 4 mmol catalyst, 20 g DI water, 200 °C, 400 psi initial pressure N₂, 1 h. For hydrothermal treatment, no glucose was added.

0.1% by adding the LaCoO₃ catalyst. The amount of solid residue decreased to 6.3% (weight percentage), which may be ascribed to the lower production yield of HMF, a notorious humin precursor in hydrothermal media. La₂O₃ and Co₂O₃ metal oxides with the same moles of La and Co ions as those of the LaCoO₃ catalyst were used for comparison. The yield of LA over Co₂O₃ reached 31.3%, which was just a little lower than that of LaCoO₃. However, after the first time usage, there was a 16.2% weight loss of Co₂O₃ due to the Co leaching, while there was almost no weight loss of LaCoO₃. La₂O₃, a weak solid base catalyst, gave only 18.8% LA yield. Approximately 20.0% of La₂O₃ dissolved in the hydrothermal media after a one-time use. (Entries 2 and 3, Table 1) Compared to the similar glucose oxidation reactions over CuO [15], the significant difference between LaCoO₃ and CuO is that no LA was produced over CuO in pH-neutral aqueous solutions, even at elevated temperatures.

3.2. Reaction temperature effect on lactic acid yield

The temperature dependence of glucose conversion with the LaCoO₃ catalyst was shown in Fig. 2. The conversion of glucose

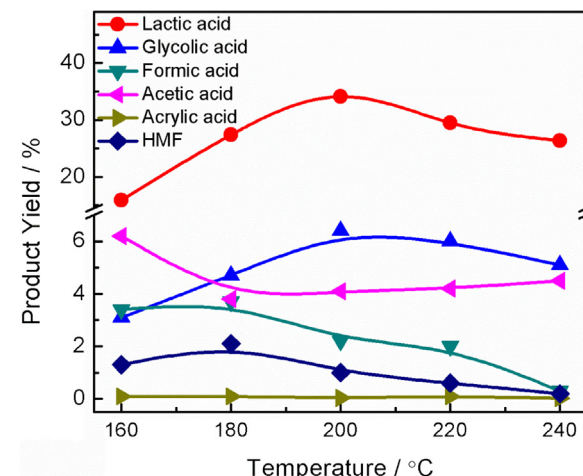


Fig. 2. Effect of reaction temperature on the glucose conversion over the LaCoO₃ catalyst in hydrothermal media. Reaction conditions: 1 mmol glucose, 0.5 mmol catalyst, 20 g DI water, 400 psi initial pressure of N₂, 1 h.

Table 1Conversions of different cellulosic biomass with and without the different catalysts^a.

Entry	Substrate	Catalyst ^b	S. R. ^b (%)	Carbon yields of aqueous products (%)							
				Gluconic	Pyruvic	Glycolic	Lactic	Formic	Acetic	HMF	Furfural
1	Glucose	/	22.2	0.9	0.4	1.8	0.9	1.9	0.0	29.1	1.1
2	Glucose	La ₂ O ₃	25.0	0.1	0.2	4.2	18.8	1.1	2.8	1.2	0.3
3	Glucose	Co ₂ O ₃	12.8	0.5	0.3	3.2	31.3	1.5	1.4	1.4	0.5
4	Glucose	LaCoO ₃	6.3	0.0	2.7	5.7	39.5	1.1	3.9	0.1	0.4
5	Glucose	Co(NO ₃) ₂	17.0	0.0	0.1	2.3	14.3	2.7	0.2	2.4	0.5
6	Fructose	/	16.6	0.3	0.2	1.7	9.8	2.4	3.4	23.1	1.1
7	Fructose	LaCoO ₃	10.4	0.0	1.4	2.3	19.8	0.6	2.6	1.4	0.6
8	Glyceraldehyde	/	39.0	–	0.6	3.2	28.9	2.3	3.2	–	–
9	Glyceraldehyde	LaCoO ₃	26.4	–	2.1	4.1	52.6	3.0	5.9	–	–
10	DHA ^c	/	34.1	–	0.6	0.0	31.9	1.4	0.8	–	–
11	DHA ^c	LaCoO ₃	29.3	–	0.4	1.6	29.8	0.8	4.5	–	–
12	Xylose	/	21.2	–	0.0	2.3	6.7	1.6	0.6	–	32.4
13	Xylose	LaCoO ₃	5.3	–	0.4	5.1	37.9	1.2	3.4	–	0.5
14 ^d	Cellulose	/	9.8	0.2	0.0	0.8	4.6	3.6	3.6	24.7	3.0
15 ^d	Cellulose	LaCoO ₃	13.6	1.6	0.5	3.3	24.9	2.4	0.8	0.3	0.1

^a Reaction conditions: 1 mmol biomass substrate, 4 mmol catalyst, 20 g DI water, 200 °C, 400 psi initial pressure of N₂, 1 h.^b S.R. represents the mass yield of solid residue.^c DHA represents 1,3 dihydroxyacetone.^d Reaction temperature is 240 °C.

increased from 85% to 98% as the reaction temperature increased from 160 °C to 200 °C, while the yield of LA enhanced from 16.0% to 34.1% and the yield of glycolic acid also increased from 3.1% to 6.4%. However, further increasing the temperature to 240 °C decreased the yield of LA to 27.4%, which might be ascribed to the degradation of LA at higher temperatures in hydrothermal media. We thus carried out a series of LA stability tests at different temperatures, as shown in Table 2. To our surprise, in the presence of the LaCoO₃ catalyst, 12% of LA was converted at 200 °C while the conversion of LA only slightly increased to 17% at 240 °C, suggesting that LA was relatively stable in subcritical water with the LaCoO₃ catalyst at <240 °C. Therefore, other side reactions might cause the decrease of the LA yield from glucose as the temperature increased from 200 °C to 240 °C.

3.3. Catalytic effect of LaCoO₃ on the conversion of other cellulosic biomass

The catalytic conversions of other carbohydrate biomass feedstocks, including C3 aldose (glyceraldehyde), C5 aldose (xylose) and polysaccharide (cellulose), were also performed using the LaCoO₃ catalyst, as shown in Entries 8, 9, 12–15, Table 1. Both C3 and C5 sugars can be converted to LA as the main product with the yields of 52.6% and 37.9% respectively, together with a considerable amount of by-products including pyruvic acid, glycolic acid, acetic acid and formic acid, which were confirmed by the GC/MS characterization

(Figs. S1–S3). The trace amounts of gluconic and xylonic acids, the characteristic intermediates produced from the partial oxidation of glucose and xylose, respectively, were also observed. Other C3 and C4 acids, such as hydroxypropionic and hydroxybutyric acids, were present as well. We found that the yield of LA from C5 xylose were very close to that from C6 glucose under the same reaction conditions. Most previous literature reports showed a retro–aldol condensation reaction pathway over the base or Lewis acid catalysed glucose conversion [14], in which one C6 glucose molecule can be cleaved to form two C3 compounds, and theoretically the yield of LA from C6 glucose can be twice higher than that from C5 xylose. The very similar LA yields from both glucose and xylose in the current study suggested a possible new reaction pathway in which retro–aldol condensation of the sugars is not the initial step of the LA formation.

It is well known that catalytic conversion of cellulose is much more challenging than converting water-soluble sugars with heterogeneous catalysts due to sluggish depolymerisation of cellulose. However, a relatively high yield of LA was obtained from cellulose at 240 °C using the LaCoO₃ catalyst. In fact, the best yield of LA, ~24.9%, in our study was higher than those using the solid Lewis acid catalysts such as ZrW and AlW [12]. The promotion function of LaCoO₃ in the conversion of cellulose might be ascribed to the lanthanide(III) ions that have a high affinity to oxygen containing functional groups in cellulose. Thus the lanthanide–saccharide

Table 2Conversion of lactic acid (LA) and gluconic acid (GA) under the different reaction conditions with and without the LaCoO₃ catalyst^a.

Entry	Substrate	Catalyst	Atmosphere	Temp.(C)	Conv. (%)	Carbon yields of aqueous products (C-%)						
						Pyruvic	Glycolic	Lactic	Formic	Acetic	Acrylic	HMF
1	LA	/	N ₂	160	1.6	0.3	0.0	–	0.1	0.1	0.0	–
2	LA	LaCoO ₃	N ₂	160	12.1	0.0	0.0	–	0.4	2.5	0.0	–
3	LA	/	N ₂	200	3.3	0.4	0.0	–	0.5	0.2	0.1	–
4	LA	LaCoO ₃	N ₂	200	12.3	0.0	0.0	–	0.2	2.8	0.0	–
5	LA	/	N ₂	240	2.0	0.6	0.0	–	0.5	0.0	0.4	–
6	LA	LaCoO ₃	N ₂	240	16.7	1.2	0.0	–	0.0	2.8	0.0	–
7	LA	/	10% O ₂	160	2.2	1.1	0.0	–	0.2	0.8	0.0	–
8	LA	LaCoO ₃	10% O ₂	160	16.6	0.8	0.0	–	0.2	4.6	0.0	–
9	LA	/	100% O ₂	240	100	0.0	0.0	–	0.0	0.0	0.0	–
10	LA	LaCoO ₃	100% O ₂	240	100	0.0	0.0	–	0.0	45.3	0.0	–
11	GA	/	N ₂	160	3.3	0.0	0.0	0.4	0.4	1.6	0.0	0.3
12	GA	LaCoO ₃	N ₂	160	13.9	0.0	0.8	5.2	1.0	4.2	0.0	0.1

^a Reaction conditions: 1 mmol biomass substrate, 0.5 mmol catalyst, 20 g DI water, 400 psi initial N₂ pressure, 1 h.

complexes formed between the hydrated lanthanide ions and the sugar units may facilitate the depolymerization of cellulose [43,44].

Furthermore, it is interesting to find that C6 fructose, an isomer of glucose, produced a much lower amount of LA than glucose over the LaCoO₃ catalyst. (Entries 6–7, Table 1) Similarly, the C3 ketose (1,3 dihydroxyacetone), the isomer of glyceraldehyde, produced a similar amount of LA over the LaCoO₃ catalyst than without catalyst, suggesting LaCoO₃ did not catalyze the conversion of dihydroxyacetone to LA. (Entries 10–11, Table 1) Note that with Lewis acid or base catalysts, ketoses, which are prone to retro-alcohol condensation, are the key intermediates in the production of LA from glucose or xylose [13,14]. However, in this study, the LaCoO₃ catalyst seemed to poorly catalyze the conversion of ketoses to LA. These results motivated us to explore the different reaction mechanism to produce LA from sugars with the LaCoO₃ catalyst.

3.4. Redox reaction mechanism

Thus far, many researchers have studied the reaction pathways of the formation of LA from sugars under hydrothermal conditions [9,10,15,45–47]. It is widely accepted that either base or Lewis acid catalysts are able to catalyse the isomerization of aldoses to ketoses and then the retro-alcohol condensation to lower-molecular weight compounds. For instance, our previous study found that the ZrO₂ catalyst containing Lewis acid/base sites promoted the retro-alcohol condensation of xylose, as well as the intramolecular Cannizzaro reaction of pyruvaldehyde, leading to the formation of LA [14].

In contrast, although the LA yield over LaCoO₃ is comparable to those over Lewis acidic zeotype catalysts [13], the Lewis acidic property of the LaCoO₃ catalyst was ruled out according to the pyridine desorption FTIR spectra as shown in Fig. 3. Moreover, the NH₃ TPD result (Fig. S4) also confirmed that the LaCoO₃ did not show Brønsted acidic property either. The basicity of the LaCoO₃ catalyst was negligible, as seen in the CO₂ TPD curve (Fig. S5). Instead, the redox properties of the LaCoO₃ were dominant. According to the TPR analysis, the hydrogen intake profile of LaCoO₃ (Fig. 4a) displayed two peaks between 300 and 500 °C and 500–700 °C which suggested a two-step reduction process: the reduction of Co³⁺ to Co²⁺ at 300–500 °C and the further reduction of Co²⁺ to Co⁰ at ~600 °C. Reverse transformation of Co ion states was observed by the TPO analysis (Fig. 4b), in which the peaks at 200–400 °C indicate the transition of Co⁰ to Co²⁺ and peaks at 700–800 °C show the oxidation from Co²⁺ to Co³⁺. The results are coincident with literature reports on the characterization of LaCoO₃ in liquid phase reaction [48]. The TPR profile of Co₂O₃ shows three main peaks with the maxima at ~360, 420 and 480 °C, indicating the reduction of Co³⁺

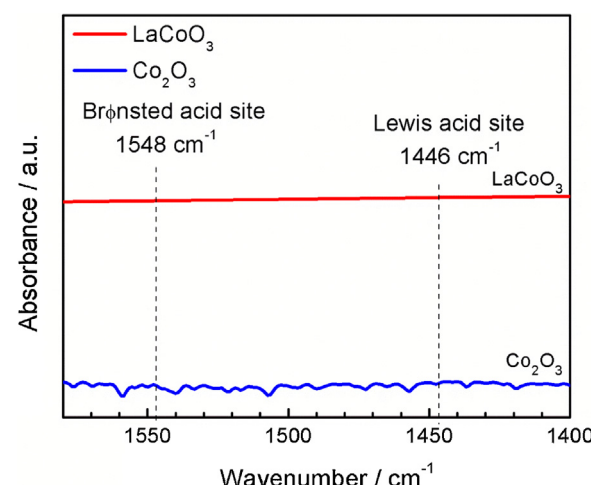


Fig. 3. FTIR spectra of adsorbed pyridine on LaCoO₃ and Co₂O₃ materials.

to Co²⁺, coexisting Co²⁺ and Co³⁺ ions as in Co₃O₄, and the further reduction of Co²⁺ to Co⁰ at ~500 °C. The TPO analysis correspondingly showed three main peaks with the maxima at ~390, 510 and 550 °C, indicating the transition of Co⁰ to Co²⁺, coexisting Co²⁺ and Co³⁺ ions, and the oxidation of Co²⁺ back to Co³⁺. The results show that the H₂ uptake capacity of Co₂O₃ was less than that of LaCoO₃ on the basis of the same moles of Co ions in both materials, which may explain why lower amounts of LA from glucose were produced over Co₂O₃ than over LaCoO₃ at the same Co loading.

To clarify the possible redox role of LaCoO₃ during the conversion of glucose to LA, the effect of different types of reaction atmospheres on the LA yield was further investigated. We found that the LA yield decreased significantly from 16.0% to 4.1% by increasing the O₂ partial pressure from 0% to ~5%, while at the same time the glycolic acid and formic acid yields increased significantly, as shown in Fig. 5a. Further increasing the O₂ partial pressure continually decreased the LA yields. Under the 100% O₂ atmosphere, only a negligible amount of LA was synthesized, compared to the yields of 22.7% glycolic acid, 8.7% formic acid and 6.9% acetic acid. On the other hand, without the LaCoO₃ catalyst, regardless of the O₂ partial pressure, LA was formed only in trace amounts. Using xylose as the feedstock, we also observed the same trend, as shown in Fig. 5b. LA was thus used as the probe to test its own stability under a wide range of O₂ partial pressures, as seen in Table 2. At 240 °C, LA is relatively stable under N₂ atmosphere and ~17% LA was converted over the LaCoO₃ catalyst. In contrast, under 100% O₂ atmosphere,

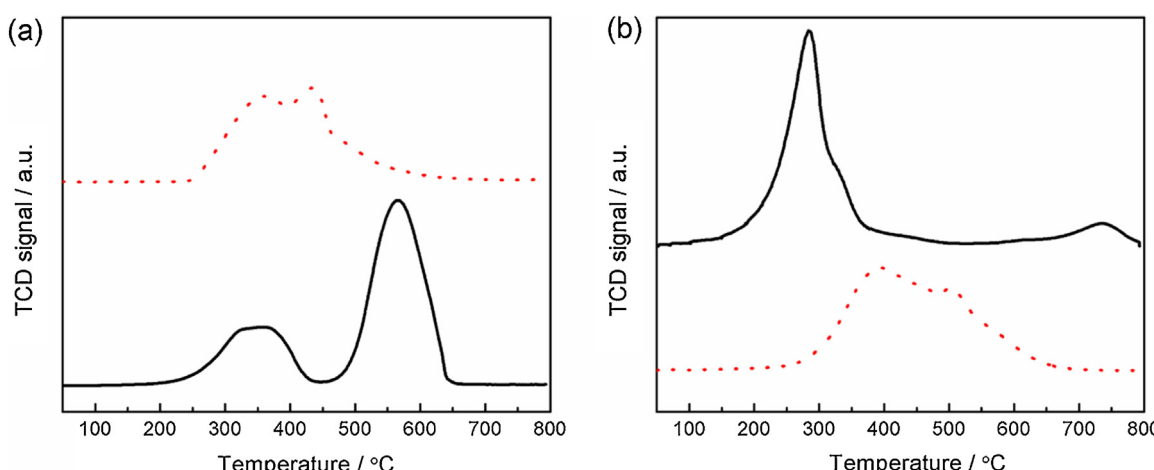


Fig. 4. (a) H₂ temperature programmed reduction (TPR) and (b) O₂ temperature programmed oxidation (TPO) of LaCoO₃ (solid line) and Co₂O₃ (dot line) materials.

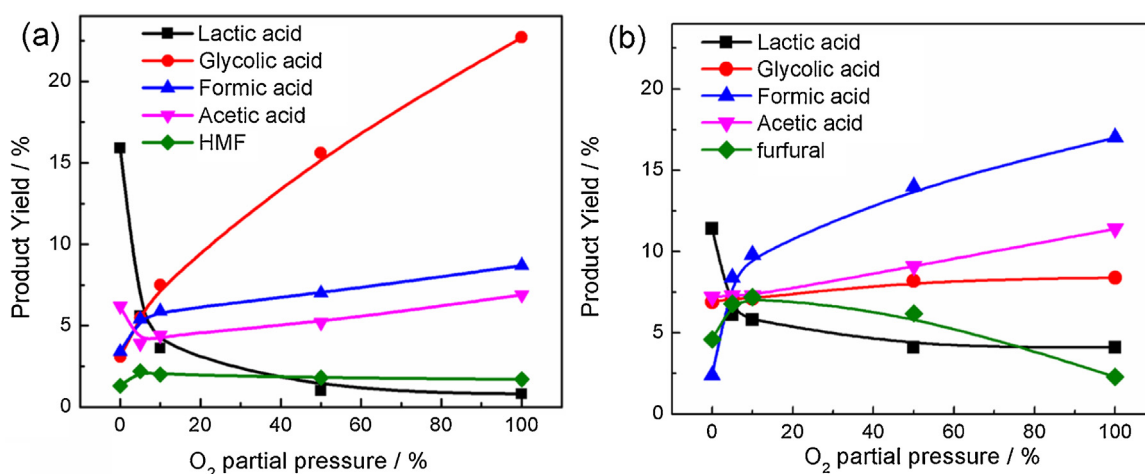


Fig. 5. Effect of O_2 partial pressure on the conversion of (a) glucose and (b) xylose over the LaCoO_3 catalyst. Reaction conditions: 1 mmol glucose or xylose, 2 mmol catalyst, 20 g DI water, 160°C , 400 psi initial pressure, 1 h.

LA was fully converted and 45% acetic acid was produced over the LaCoO_3 catalyst. Very interestingly, adding a small amount of H_2 in N_2 atmosphere seemed to have a minor promotional effect, or at least no inhibition effect like O_2 , on the conversion of glucose to LA in the presence of high loadings of the LaCoO_3 catalyst. Compared to the pure N_2 atmosphere, the LA yield slightly changed from 39.5% to 40.1% with adding 5.5% of H_2 into N_2 . The conversion of glucose to LA over the LaCoO_3 catalyst might proceed through an initial step of partial oxidation of glucose which was performed better in N_2 than in O_2 . Under the pure N_2 atmosphere, LaCoO_3 is the possible weak oxidant that selectively oxidized glucose.

We thus propose a possible redox reaction mechanism (**Scheme 1**) with the hypothesis that oxygen for the oxidation reactions during the conversion of glucose to LA might be stemmed from the lattice oxygen atoms in the LaCoO_3 perovskite structure, similar to the classical Mars and Van Krevelen (MvK) mechanism, i.e., lattice oxygen of metal oxide takes part in oxidation reactions, which is widely accepted in gas-phase oxidation processes but rarely reported in aqueous-phase oxidation processes [49,50]. Here, the oxygen atoms in the lattice of LaCoO_x might participate in the redox cycles of the transformation of glucose and its derived intermediates. For instance, LaCoO_3 firstly oxidizes the aldehyde group in glucose to form gluconic acid, which is different from isomerization and retro-aldo condensation as the initial step of acid/base catalysed glucose conversion reactions [14]. The catalyst itself is reduced from LaCoO_3 to $\text{LaCoO}_{2.5}$ and the corresponding cobalt valence states changed from Co^{3+} to Co^{2+} . Afterwards, gluconic acid undergoes an oxidative decarboxylation [51] and is transformed to xylose, which was detected by the GC-MS (Fig. S1b). Xylose repeats the oxidation step to form xylonic acid and then undergoes oxidative decarboxylation to produce C4 aldose, which is then oxidized to hydroxybutyric acid. Finally hydroxypropionic acid is formed by the alternate oxidative decarboxylation and oxidation. Hydroxypropionic acid can continue to react in the same fashion to further produce glycolic acid and then formic acid, especially with the presence of strong oxidants like O_2 , as we observed that under higher O_2 partial pressures, more glycolic and formic acids, rather than LA, were produced from glucose. On the other hand, hydroxypropionic acid can also undergo a dehydration reaction at elevated temperatures to produce pyruvic acid, which was also detected by the GC-MS. It is possible that over the reduced perovskite structure, $\text{LaCoO}_{2.5}$, pyruvic acid is reduced to LA. Meanwhile, Co^{2+} is oxidised back to Co^{3+} and complete the catalytic cycle of $\text{Co}^{3+} \rightarrow \text{Co}^{2+} \rightarrow \text{Co}^{3+}$, while the perovskite structure is unchanged.

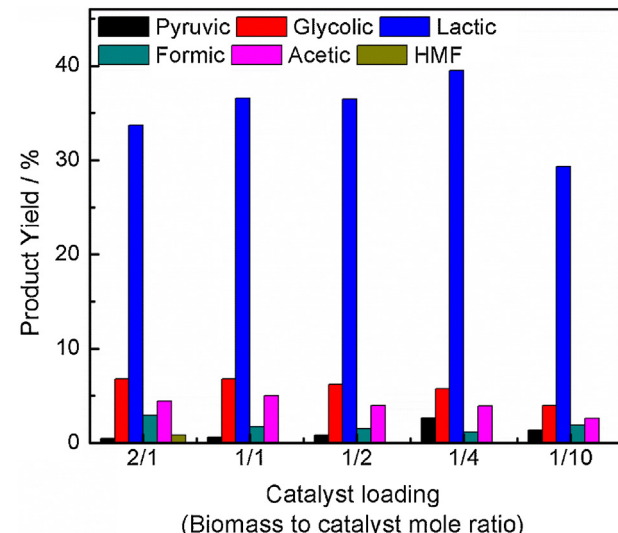
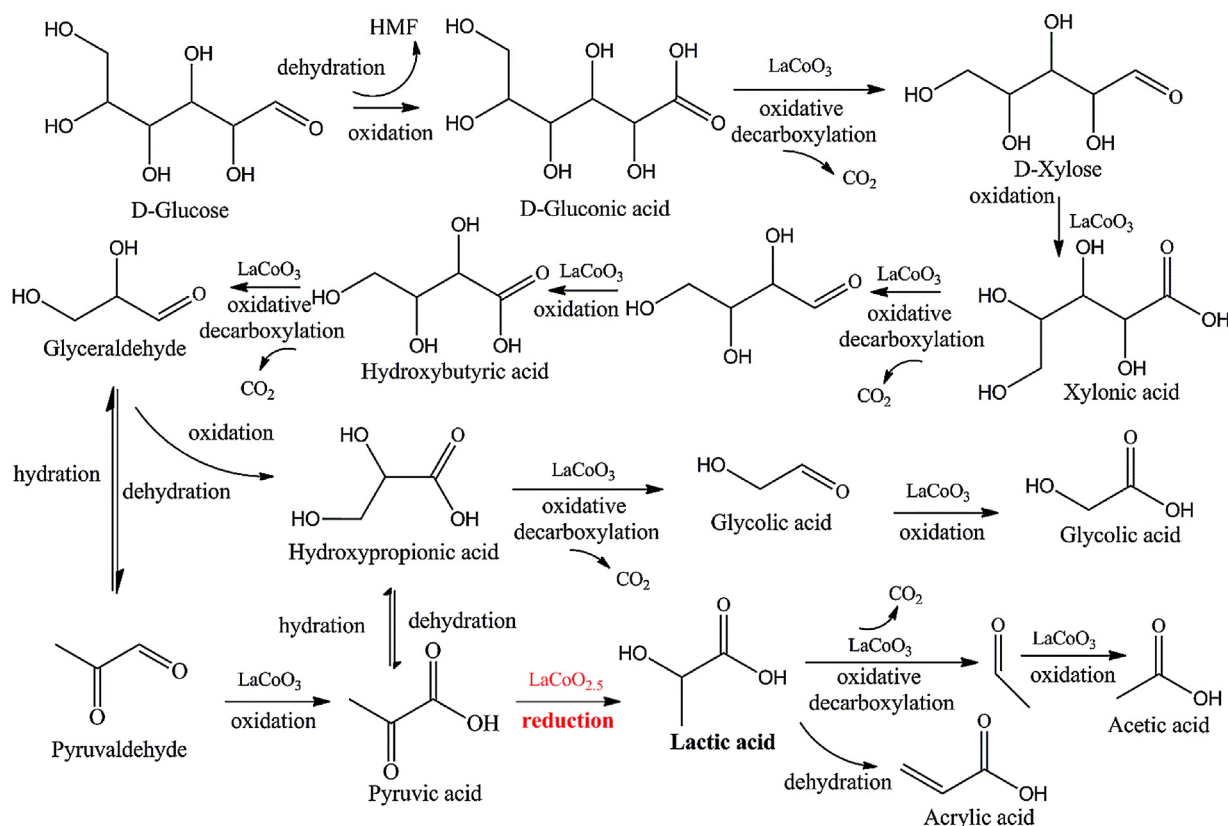


Fig. 6. Effect of catalyst loading amount on the product yields of the glucose conversion over the LaCoO_3 catalyst. Reaction conditions: 1 mmol glucose, 20 g DI water, 200°C , 400 psi initial pressure of N_2 , 1 h.

To test our hypothesis that LaCoO_3 serves as the weak oxidant, we examined the effects of different catalyst loading amounts on the LA yield. As shown in **Fig. 6**, by increasing the molar ratio of LaCoO_3 to glucose from 0.5:1 to 4:1, the LA yield increased from ~33% to ~40%. However, as the catalyst to biomass molar ratio further increased to 10:1, the LA yield decreased significantly to ~32%. These results reasonably support our hypothesis: stoichiometrically one mole of LaCoO_3 only provides 0.5 moles of oxygen, but there are multiple oxidation steps during the conversion of glucose to LA, and thus excess catalyst loadings are needed to achieve a high yield of LA. However, as the molar ratio of catalyst to glucose was too high, the excess LaCoO_3 might prevent $\text{LaCoO}_{2.5}$ from reducing pyruvic acid, the key step to produce LA in our proposed mechanism.

To further illustrate this key redox step, pyruvic acid was used as a probe reactant to find out whether it would be reduced over the LaCoO_3 catalyst which was pre-reduced with the H_2 flow. We found that in the pure N_2 atmosphere, a yield of 16.5% LA was obtained from pyruvic acid without adding any catalyst at 200°C , while 21.3% glycolic acid was the dominant product. In contrast, 36.8% LA was produced as the dominant product over the pre-reduced LaCoO_3 .



Scheme 1. Proposed redox reaction pathway for the formation of lactic acid from glucose with the LaCoO_3 catalyst.

catalyst. In addition, when supplementary H_2 was added into the N_2 atmosphere, a 56.9% LA yield was obtained, as shown in Table 3. This is in contrast to the conversion of pyruvic acid to LA with the fully oxidized LaCoO_3 , over which only a 3.6% LA yield was obtained.

We also used gluconic acid as the probe reactant to validate the proposed reaction mechanism. At 200°C , 14% gluconic acid was converted, with LA and acetic acid as the dominant products (Entry 12, Table 2). The probe reaction results suggest that the proposed reaction pathway is reasonable although the actual chemistry and kinetics could be much more complex in this reaction system. Similarly, other aldoses such as xylose undergo the same redox cycles to produce LA. The stepwise oxidative decarboxylation of the aldoses, with the different carbon numbers ranging from six to four, peels off the carbon in the end aldehyde group to form CO_2 . According to our proposed redox reaction mechanism, ideally, 1 mmol of glucose will produce 1 mmol of LA and 3 mmol of CO_2 . In the typical glucose conversion experiment, 3.12 mmol of CO_2 were produced from 1 mmol of glucose, as seen in Fig. S6. The carbon balance of this reaction was close to 100%. As this reaction proceeds, CO_2 would be the only end product. Indeed, it is unclear why LA is more sta-

ble products compared to other C1 and C2 acids. However, this proposed redox reaction mechanism well explained why the production yields of LA from xylose were nearly the same as those from glucose. On the other hand, ketose such as fructose, which possesses the end ketone group instead of the end aldehyde group, is recalcitrant to the oxidative decarboxylation and thus hardly produces as a high amount of LA as glucose over the LaCoO_3 catalyst.

3.5. Stability of LaCoO_3 catalyst

We found that the stability of either La_2O_3 or Co_2O_3 was poor under hydrothermal conditions, while the perovskite structure of LaCoO_3 stabilized La and Co ions to some extent. Our catalyst stability was examined by five consecutive usages of the fresh and spent LaCoO_3 catalysts for the conversion of glucose to LA. The spent catalyst after each use was regenerated by calcination in air at 550°C for 6 h in order to remove any biomass derived solid residues. Fig. 7 shows that the yield of LA decreased from 39.5% to 33.3% after the first usage. The activity of the spent LaCoO_3 catalyst was restored after the regeneration and remained fairly stable

Table 3

Conversion of pyruvic acid with and without the different LaCoO_3 catalysts under inert or reductive atmospheres.

Entry	Catalyst	B/C ^b	Atm.	Carbon yields of aqueous products (C-%) ^a			
				Glycolic	Lactic	Formic	Acetic
1	–	–	N_2	21.3	16.5	0.8	2.5
2	R. LaCoO_3	1/2	N_2	3.8	36.8	0.1	3.2
3	O. LaCoO_3	1/2	N_2	24.5	3.6	0.0	1.6
4	–	–	H_2 and N_2 ^c	19.7	17.2	0.7	3.3
5	R. LaCoO_3	1/2	H_2 and N_2 ^c	0.0	56.9	0.0	4.8

^a Reaction conditions: 1 mmol pyruvic acid, 2 mmol pre-reduced (R.) or fully oxidized (O.) LaCoO_3 catalyst, 200°C , 400 psi initial pressure, 1 h.

^b B/C represents the mole ratio of biomass substrate to catalyst.

^c A mixture of H_2 and N_2 atmosphere with 2 mmol H_2 .

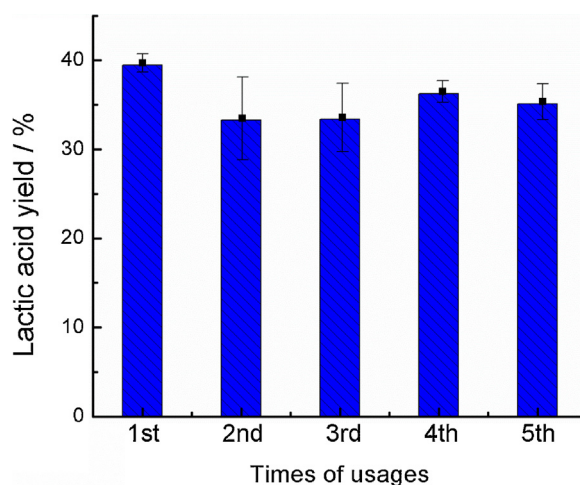


Fig. 7. Stability of the LaCoO₃ catalyst in the production of lactic acid from glucose in hydrothermal media. Reaction conditions: 1 mmol glucose, 4 mmol catalyst, 20 g DI water, 200 °C, 400 psi initial pressure of N₂, 1 h. For the 4th and 5th reactions, the feed amounts of glucose were slightly adjusted in order to keep the same ratio of catalyst to glucose.

through the following usages after the first reuse in the hydrothermal reaction system. In contrast, the yield of LA decreased to less than 20% with the un-regenerated catalyst. During the reaction, the LaCoO₃ catalyst acted as an oxidant initially; after reaction, it was mostly reduced while only part of LaCoO₃ were restored to the oxidized state by the reduction of pyruvic acid. That is why the catalyst activity is low if we reuse the spent LaCoO₃ catalyst without regeneration. However, after being calcined in air, the spent catalyst was fully oxidized again and thus the catalytic activity was restored. Hence, unlike other catalysts, LaCoO₃ in this reaction is similar to a recyclable solid reactant.

The XRD analysis shows that after the 1-h treatment in the pH neutral hydrothermal medium at 200 °C, the crystalline structure of LaCoO₃ was almost unchanged (Fig. 1b). However, after the 1-h glucose conversion reaction, a slight collapse of crystalline structure of the LaCoO₃ catalyst was observed, as shown in Fig. 1c. The pH of the aqueous solution decreased to 3.75 after the reaction due to the formation of carboxylic acids, which might accelerate the leaching of metal ions. Elemental analysis by EDS confirmed that a small amount of Co ions in the LaCoO₃ was leached out after the reaction compared with the fresh sample, as shown in Fig. S7. Additionally, the leaching of Co and La during the typical reaction (after the first use of the LaCoO₃ catalyst in Fig. 7) was characterized by the inductively coupled plasma atomic emission spectroscopy (ICP-AES). Approximately 2.4 mol% Co ions and 1.5 mol% La ions were leached out from the LaCoO₃ perovskite catalyst after the reaction. Yet the Co and La ions leached out from the Co₂O₃ and La₂O₃ catalysts were ~11.4 mol% and ~15.0 mol% respectively in the control reactions under the otherwise identical conditions. Although the structure of perovskite could not completely prevent the leaching of Co and La ions, it significantly retarded the leaching process.

The leached Co ions might be the homogeneous Lewis acid which could potentially catalyse the production of LA from sugars. The comparative tests using Co²⁺ as catalyst were thus carried out to determine whether or not the catalytic performance was stemmed from the leached Co ions. Different product distributions and LA yields were observed when using the equal moles of Co(NO₃)₂ and LaCoO₃ as the catalysts, respectively (Entry 5, Table 1). The Co²⁺ ion promoted the dehydration of glucose as a noticeable yield of HMF (2.4%) was produced which was not observed by using the LaCoO₃ catalyst. Yet the yield of LA with the Co(NO₃)₂ catalyst was ~14% which was much lower than that of

~40% LA using the LaCoO₃ catalyst. Therefore the leached Co ions did not dominantly catalyse the LA formation during the catalytic conversion of sugars in the presence of the LaCoO₃.

The changes in particle size, surface composition, and surface area were dynamic in the reactive environment. We found the mean crystallite size of LaCoO₃ decreased from ~77.2 nm to ~48.3 nm (calculated from the XRD spectra) after the 1st reaction. The decrease of the size could certainly increase the surface area. However, since the BET surface area of the fresh LaCoO₃ material was already rather low (Table S1), the effect of surface area change might be minimal. Note that the LA yield decreased from 39.5% to 33.3% after the 1st use and then remained stable throughout the subsequent re-use of the spent catalyst, as shown in Fig. 7, suggesting that the dominant factor might be leaching instead of the changes in particle size or surface area and leaching might be reversible under the reaction condition.

4. Conclusions

In summary, we demonstrate that the LaCoO₃ perovskite catalyst can effectively catalyse the conversion of cellulosic biomass to lactic acid in hydrothermal media. The reaction temperature, gas atmosphere, and catalyst loading had profound effects on the production yield of lactic acid from glucose. C5 to C6 aldose sugars including xylose and glucose yielded a similar amount of lactic acid, up to ~40%, at 200 °C and the initial pressure of 400 psi N₂, while the highest yield of lactic acid from cellulose was ~24% at 240 °C, in hydrothermal media. Much lower amounts of HMF and humin products were obtained from glucose with the LaCoO₃ catalyst. A possible redox reaction mechanism, which involved the key steps such as the oxidative decarboxylation of aldose sugars and the reduction of pyruvic acid with the aid of the Co³⁺ and Co²⁺ redox cycles in the LaCoO₃ perovskite structure, was proposed for the conversion of aldose sugars to lactic acid. Unlike Lewis acid or base catalysed reactions in which the production of lactic acid was initialized by the retro-alcohol condensation of the sugars, the lattice oxygen atoms in the LaCoO₃ perovskite metal oxides acted as the weak oxidants in the selective conversions of aldoses to lactic acid under inert or even mild reductive atmosphere. The leaching of LaCoO₃ occurred during the glucose conversion reactions in hydrothermal media but the catalyst was found to be relatively stable in the short term.

Acknowledgements

We gratefully thank Prof. Glenn Miller for the useful discussion, Dr. Stevens Spain at the Shared Instrumentation Laboratory (SIL) of Chemistry department at University of Nevada Reno for the help on chemical analysis, Prof. Wei Fan at University of Massachusetts Amherst for the help on FTIR characterization, Dr. Jingji Zhang for useful discussions on the catalyst synthesis, and Mr. Reed Nicholas Liu for proofreading. This material is based upon work supported by the National Science Foundation under Grant no. CBET 1337017.

Appendix A. Supplementary data

Supplementary data associated with this article can be found, in the online version, at <http://dx.doi.org/10.1016/j.cattod.2015.12.003>.

References

- [1] A. Milbrandt, A geographic perspective on the current biomass resource availability in the United States, NREL Tech. Rep. NREL/TP-56 (2005) 1–50.
- [2] A. Corma, S. Iborra, A. Velty, Chemical routes for the transformation of biomass into chemicals, *Chem. Rev.* 107 (2007) 2411–2502.

- [3] M. Dusselier, P. Van Wouwe, A. Dewaele, E. Makshina, B.F. Sels, Lactic acid as a platform chemical in the biobased economy: the role of chemocatalysis, *Energy Environ. Sci.* 6 (2013) 1415–1442.
- [4] D. Garlotta, A literature review of poly (lactic acid), *J. Polym. Environ.* 9 (2002) 63–84.
- [5] A. Higson, Lactic acid, *Renew. Chem. Factsheet* (2011) 1–2.
- [6] Rojan P. John, G.S. Anisha, K. Madhavan Nampoothiri, Ashok Pandey, Direct lactic acid fermentation: focus on simultaneous saccharification and lactic acid production, *Biotechnol. Adv.* 27 (2009) 145–152.
- [7] C. Gao, C. Ma, P. Xu, Biotechnological routes based on lactic acid production from biomass, *Biotechnol. Adv.* 29 (2011) 930–939.
- [8] A. Onda, T. Ochi, K. Kajiyoshi, K. Yanagisawa, A new chemical process for catalytic conversion of D-glucose into lactic acid and gluconic acid, *Appl. Catal. A Gen.* 343 (2008) 49–54.
- [9] L. Kong, G. Li, H. Wang, W. He, F. Ling, Hydrothermal catalytic conversion of biomass for lactic acid production, *J. Chem. Technol. Biotechnol.* 83 (2008) 383–388.
- [10] X. Yan, F. Jin, K. Tohji, A. Kishita, H. Enomoto, Hydrothermal conversion of carbohydrate biomass to lactic acid, *AIChE J.* 56 (2010) 2727–2733.
- [11] G. Epane, J.C. Laguerre, A. Wadouachi, D. Marek, Microwave-assisted conversion of D-glucose into lactic acid under solvent-free conditions, *Green Chem.* 12 (2010) 502.
- [12] F. Chambon, F. Rataboul, C. Pinel, A. Cabiac, E. Guillou, N. Essayem, Cellulose hydrothermal conversion promoted by heterogeneous Brønsted and Lewis acids: Remarkable efficiency of solid Lewis acids to produce lactic acid, *Appl. Catal. B Environ.* 105 (2011) 171–181.
- [13] M.S. Holm, S. Saravananurugan, E. Taarning, Conversion of sugars to lactic acid derivatives using heterogeneous zeotype catalysts, *Science* 328 (2010) 602–605.
- [14] L. Yang, J. Su, S. Carl, J.G. Lynam, X. Yang, H. Lin, Catalytic conversion of hemicellulosic biomass to lactic acid in pH neutral aqueous phase media, *Appl. Catal. B Environ.* 162 (2015) 149–157.
- [15] Y. Wang, F. Jin, M. Sasaki, F. Wang, Z. Jing, M. Goto, Selective conversion of glucose into lactic acid and acetic acid with copper oxide under hydrothermal conditions, *AIChE J.* 59 (2013) 2096–2104.
- [16] F.F. Wang, J. Liu, H. Li, C.L. Liu, R.Z. Yang, W.S. Dong, Conversion of cellulose to lactic acid catalyzed by erbium-exchanged montmorillonite K10, *Green Chem.* 17 (2015) 2455–2463.
- [17] R.M. West, M.S. Holm, S. Saravananurugan, J. Xiong, Z. Beversdorf, E. Taarning, et al., Zeolite H-USY for the production of lactic acid and methyl lactate from C3-sugars, *J. Catal.* 269 (2010) 122–130.
- [18] R. Datta, M. Henry, Lactic acid: recent advances in products, processes and technologies – a review, *J. Chem. Technol. Biotechnol.* 81 (2006) 1119–1129.
- [19] S. Tolborg, I. Sádaba, C.M. Osmundsen, P. Fristrup, M.S. Holm, E. Taarning, Tin-containing silicates: alkali salts improve methyl lactate yield from sugars, *ChemSusChem* 8 (2015) 613–617.
- [20] Z. Liu, W. Li, C. Pan, P. Chen, H. Lou, X. Zheng, Conversion of biomass-derived carbohydrates to methyl lactate using solid base catalysts, *Catal. Commun.* 15 (2011) 82–87.
- [21] E.F. Glynna, L. Li, Supercritical water oxidation research and development update, *Environ. Prog.* 14 (1995) 182–192.
- [22] K. Tomita, Y. Oshima, Stability of manganese oxide in catalytic supercritical water oxidation of phenol, *Ind. Eng. Chem. Res.* 43 (2004) 7740–7743.
- [23] M. Watanabe, H. Inomata, K. Arai, Catalytic hydrogen generation from biomass (glucose or cellulose) with ZrO₂ in supercritical water, *Biomass Bioenergy* 22 (2002) 405–410.
- [24] J. Yu, P.E. Savage, Catalyst activity, stability, and transformations during oxidation in supercritical water, *Appl. Catal. B Environ.* 31 (2001) 123–132.
- [25] C.C. Chang, H.S. Weng, Deep oxidation of toluene on perovskite catalyst, *Ind. Eng. Chem. Res.* 32 (1993) 2930–2933.
- [26] M.A. Peña, J.L.G. Fierro, Chemical structures and performance of perovskite oxides, *Chem. Rev.* 101 (2001) 1981–2017.
- [27] U. Singh, J. Li, J. Bennett, A. Rappe, R. Seshadri, S. Scott, A Pd-doped perovskite catalyst, BaCe_{1-x}PdxO_{3-δ}BaCe_{1-x}PdxO_{3-δ}, for CO oxidation, *J. Catal.* 249 (2007) 349–358.
- [28] G. Valderrama, A. Kiennemann, M.R. Goldwasser, La–Sr–Ni–Co–O based perovskite-type solid solutions as catalyst precursors in the CO₂ reforming of methane, *J. Power Sources* 195 (2010) 1765–1771.
- [29] S.M. de Lima, A.M. da Silva, L.O.O. da Costa, J.M. Assaf, L.V. Mattos, R. Sarkari, et al., Hydrogen production through oxidative steam reforming of ethanol over Ni-based catalysts derived from La_{1-x}Ce_xNiO₃ perovskite-type oxides, *Appl. Catal. B Environ.* 121–122 (2012) 1–9.
- [30] C. Pichas, P. Pomonis, D. Petrakis, A. Ladavos, Kinetic study of the catalytic dry reforming of CH₄ with CO 2 over La_{2-x}SrxNiO₄ perovskite-type oxides, *Appl. Catal. A Gen.* 386 (2010) 116–123.
- [31] G. Valderrama, C. Urbina de Navarro, M.R. Goldwasser, CO₂ reforming of CH₄ over Co-La-based perovskite-type catalyst precursors, *J. Power Sources* 234 (2013) 31–37.
- [32] J. Chen, M. Shen, X. Wang, G. Qi, J. Wang, W. Li, The influence of nonstoichiometry on LaMnO₃ perovskite for catalytic NO oxidation, *Appl. Catal. B Environ.* 134–135 (2013) 251–257.
- [33] J. Chen, M. Shen, X. Wang, J. Wang, Y. Su, Z. Zhao, Catalytic performance of NO oxidation over LaMeO₃ (Me=Mn, Fe, Co) perovskite prepared by the sol-gel method, *Catal. Commun.* 37 (2013) 105–108.
- [34] Y.-H. Dong, H. Xian, J.-L. Lv, C. Liu, L. Guo, M. Meng, et al., Influence of synthesis conditions on NO oxidation and NO_x storage performances of La_{0.7}Sr_{0.3}MnO₃ perovskite-type catalyst in lean-burn atmospheres, *Mater. Chem. Phys.* 143 (2014) 578–586.
- [35] M. Markova-Velikhova, T. Lazarova, V. Tumbalev, G. Ivanov, D. Kovacheva, P. Stefanov, et al., Complete oxidation of hydrocarbons on YFeO₃ and LaFeO₃ catalysts, *Chem. Eng. J.* 231 (2013) 236–244.
- [36] H. Najjar, H. Batis, La–Mn perovskite-type oxide prepared by combustion method: catalytic activity in ethanol oxidation, *Appl. Catal. A Gen.* 383 (2010) 192–201.
- [37] W.P. Stege, L.E. Cadús, B.P. Barbero, La_{1-x}CaxMnO₃ perovskites as catalysts for total oxidation of volatile organic compounds, *Catal. Today* 172 (2011) 53–57.
- [38] H. Deng, L. Lin, Y. Sun, C. Pang, J. Zhuang, P. Ouyang, et al., Perovskite-type oxide LaMnO₃: an efficient and recyclable heterogeneous catalyst for the wet aerobic oxidation of lignin to aromatic aldehydes, *Catal. Lett.* 126 (2008) 106–111.
- [39] H. Deng, L. Lin, Y. Sun, C. Pang, J. Zhuang, P. Ouyang, et al., Activity and stability of perovskite-type oxide LaCoO₃ catalyst in lignin catalytic wet oxidation to aromatic aldehydes process, *Energy Fuels* 23 (2009) 19–24.
- [40] H. Deng, L. Lin, S. Liu, Catalysis of Cu-doped Co-based perovskite-type oxide in wet oxidation of lignin to produce aromatic aldehydes, *Energy Fuels* 24 (2010) 4797–4802.
- [41] N. Escalona, W. Aranzaez, K. Leiva, N. Martínez, G. Pecchi, Ni nanoparticles prepared from Ce substituted LaNiO₃ for the guaiacol conversion, *Appl. Catal. A Gen.* 481 (2014) 1–10.
- [42] H. Li, S. Wang, W. Wang, J. Ren, F. Peng, R. Sun, et al., One-step heterogeneous catalytic process for the dehydration of xylan into furfural, *Bioresources* 8 (2013) 3200–3211.
- [43] K. Seri, Y. Inoue, H. Ishida, Catalytic activity of lanthanide(III) ions for the dehydration of hexose to 5-hydroxymethyl-2-furaldehyde in water, *Bull. Chem. Soc. Jpn.* 74 (2001) 1145–1150.
- [44] H. Ishida, K. Seri, Catalytic activity of lanthanoid III ions for dehydration of D-glucose to 5 (hydroxymethyl) furfural, *J. Mol. Catal. A Chem.* 112 (1996) L163–L165.
- [45] M. Bicker, S. Endres, L. Ott, H. Vogel, Catalytical conversion of carbohydrates in subcritical water: a new chemical process for lactic acid production, *J. Mol. Catal. A Chem.* 239 (2005) 151–157.
- [46] X. Lei, F.-F. Wang, C.-L. Liu, R.-Z. Yang, W.-S. Dong, One-pot catalytic conversion of carbohydrate biomass to lactic acid using an ErCl₃ catalyst, *Appl. Catal. A Gen.* 482 (2014) 78–83.
- [47] J. Zhang, B. Hou, A. Wang, Z. Li, H. Wang, T. Zhang, Kinetic study of retro-aldol condensation of glucose to glycolaldehyde with ammonium metatungstate as the catalyst, *AIChE J.* 60 (2014) 3804–3813.
- [48] J. Deng, L. Zhang, H. Dai, C.-T. Au, In situ hydrothermally synthesized mesoporous LaCoO₃/SBA-15 catalysts: high activity for the complete oxidation of toluene and ethyl acetate, *Appl. Catal. A Gen.* 352 (2009) 43–49.
- [49] C. Doornkamp, V. Ponec, The universal character of the Mars and Van Krevelen mechanism, *J. Mol. Catal. A Chem.* 162 (2000) 19–32.
- [50] E.M. Grieco, C. Gervasio, G. Baldi, Lanthanum–chromium–nickel perovskites for the catalytic cracking of tar model compounds, *Fuel* 103 (2013) 393–397.
- [51] W.S. Trahanovsky, J. Cramer, D.W. Brixius, Oxidation of organic compounds with cerium (IV)-oxidative decarboxylation of substituted phenylacetic acids, *J. Am. Chem. Soc.* 96 (1974) 1077–1081.